Lethaia
AN INTERNATIONAL JOURNAL OF PALAEONTOLOGY AND STRATIGRAPHY

Early Cretaceous pterosaur guano deposit from central Oregon, USA

GREGORY J. RETALLACK, GREGORY E. CARR AND ADRIAN P. BROZ

LETHAIA

Excavation of a green breccia lens in the otherwise shaley Hudspeth Formation of central Oregon recovered a surprising variety of fossils of different kinds: plant impressions, mollusc shells, and vertebrate bones and teeth. Some ammonites, such as *Mortoniceras inflatum*, which date the deposit as late Albian (103 Ma), were preserved with shell intact below, but dissolved above back to sutures. Intact ammonites were outnumbered by angular ammonite fragments in the size range 1–2 cm. Marine clams, snails and ammonites were found in the same bed as a variety of fossil plants, including horsetails, ferns, cycads, and conifers. Also recovered were bones of fish, ichthyosaurs, dinosaurs, and pterosaurs. Orientation of large fossil logs and branches reveal derivation from the east, where a shoreline of shingle beaches and alluvial fans created the interfingering Gable Creek Conglomerate. The matrix-supported green breccia is massive and ungraded, and interpreted as a mass flow deposit. Enrichment in phosphorus compared with shale above and below is evidence that its fine-grained component includes guano. This guano and unusual fragmentation of ammonites are interpreted as evidence that the Oregon pterosaur, *Bennettazhia oregonensis*, was a mollusc-eater and formed large colonies on nearby cliffs, like modern gull rookeries.
□ *Cretaceous, Oregon, guano, pterosaur, debris flow, Hudspeth Formation*

Gregory J. Retallack ✉ [gregr@uoregon.edu] and Adrian P. Broz [abroz@uoregon.edu], Department of Earth Sciences, University of Oregon, Eugene, Oregon 97302 USA; Gregory E. Carr [gpcarr@comcast.net], 8217 SW Hemlock St, Portland, Oregon 97223: *manuscript received on 15/02/2022; manuscript accepted on 20/10/2022; manuscript published on 21/02/2023 in* Lethaia 56(1).

Fossil assemblages reflect particular communities of plants, invertebrates or vertebrates, but seldom all of these together. This is because taphonomic constraints of low Eh and pH needed for fossil plants exclude much bone and shell, and high Eh and pH for shell and bone beds excludes fossil plant preservation (Retallack 1984). There are exceptions to this rule if the deposit were quarried extensively and long enough to find rarities (Barthel *et al.* 1990; Frigo & Sorbini 1999; Smith *et al.* 2018), or if an entire ecosystem were buried catastrophically (Retallack 1992; Baumgartner & Peppe 2021) in a manner comparable with the destruction of the Ancient Roman town of Pompei (Jashemski & Meyer 2002). An intriguing fossil bed in the Early Cretaceous Hudspeth Shale of central Oregon with equally abundant different kinds of fossils, including plant impressions, shells, bone and teeth (Table 1), presents an exception to taphonomy as usual. In addition, some of the ammonites were broken before deposition into exceptionally small angular fragments, and new bones were found of the rare Oregon pterosaur *Bennetazhia oregonensis* (Gilmore 1928; Nesov 1991). These intriguing new discoveries are incorporated into a novel interpretation of an unusual bed in the Early Cretaceous, Hudspeth Formation of Oregon.

Geological setting

The excavation site is locality UO13522 of the Museum of Natural and Cultural History of the University of Oregon, on a gentle ridge of shale on public lands administered by the Bureau of Land Management, 3 miles northwest of Mitchell, Wheeler County, Oregon, at N44.60256º W120.17297º (Fig. 1). The locality is within the main mudstone member of the Hudspeth Formation at a stratigraphical level of 375 m in the measured section (Fig. 2) of Wilkinson & Oles (1968). Three distinct members of the Hudspeth include: 1, basal member of sandstone interpreted as former beaches and rivers; 2, main mudstone member of fossiliferous shale interpreted as a shallow marine continental shelf; and 3, upper member of poorly fossiliferous graded beds interfingering with Gable Creek Formation, interpreted as turbidites of a submarine fan and canyon complex (Kleinhans *et al.* 1984; Hausen & Dorsey, 2005; Dorsey & Lenegan 2007). The biostratigraphical age of the Hudspeth Formation is Albian to Cenomanian, but the excavated section is late early Albian, within the endemic *Brewericeras hulenense* ammonite zone (Jones *et al.* 1965). Cosmopolitan ammonites also are found near the Mitchell locality, which is stratigraphically above

https://doi.org/10.18261/let.56.1.3

Table 1. List of fossil species from the excavated green breccia of the Hudspeth Formation

Category	Taxon	Species	Reference	example
horsetail	Equisetaceae	*Equisetum burchardtii*	Skog & Dilcher 1994	Fig.9A
fern	Marattiaceae	*Nathorstia angustifolia*	Kvaček & Dašková 2007	Fig.9B
cycad	Cycadaceae	*Nilssonia schaumburgensis*	Bell 1956	Fig.9D
cycad	Cycadaceae	*Nilssonia canadensis*	Bell 1956	Fig.9C
cycad	Cycadaceae	*Cycadeospermum lineatum*	Berry 1922	Fig.9E,F
conifer	Pinaceae	*Margeriella cretacea*	Page 1973	Fig.9G,L
conifer	Cupressaceae	*Cyparissidium gracile*	Bell 1956	Fig.9H
conifer	Taxodiaceae	*Elatocladus smittianus*	Bell 1956	Fig.9K
conifer	Taxodiaceae	*Elatides splendida*	Bell 1956	Fig.9I,J
clam	Buchiidae	*Aucellina dowlingi*	Imlay 1961	F127950
clam	Inoceramidae	*Actinoceramus concentricus*	Jones 1960	F127905
clam	Astartidae	*Opis popenoei*	Squires & Saul 2009	F127904
clam	Pholadidae	*Teredolites clavatus*	Bromley *et al.* 1984	F127911
snail	Aporrhaidae	*Anchura biangulata*	Anderson 1938	F127953
snail	Pseudomelaniidae	*Pseudomelania colusaensis*	Anderson 1958	F118846
nautilid	Cymatoceratidae	*Cymatoceras carlottense*	Miller & Harris, 1945	F127952
ammonite	Cleoniceratidae	*Brewericeras hulenense*	Jones *et al*. 1965	F127929
ammonite	Brancoceratidae	*Mortoniceras inflatum*	Lehman 2015	Fig.7E
ammonite	Anisoceratidae	*Anisoceras merriami*	Packard & Jones 1962	F127949
ammonite	Desmoceratidae	*Desmoceras alamoense*	Gautam et al. 2019	F127898
ammonite	Desmoceratidae	*Desmoceras latidorsatum*	Kawabe & Haggart 2003	F127899
ammonite	Desmoceratidae	*Puzosia dilleri*	Anderson 1938	F127900
ammonite	Tetragonitidae	*Tetragonites hulenensis*	Murphy 1967	F127901
ammonite	Baculitidae	*Lechites comanchensis*	Clark 1965	F127902
echinoid	Cidaridae	*Paracidaris* sp. indet.	Smith & Rader, 2009	F127907
echinoid	Cidaridae	smooth narrow spines indet.	Smith & Rader, 2009	F127906
barnacle	Balanidae	Plates indet.		F127922
fish	Teleostei	Skull bones, vertebrae, ribs		F127909
shark	Mitsukurinidae	*Scapanorhynchus* sp. indet.	Welton 1972	F127701
shark	Otodontidae	*Cretalamna* sp. indet.	Siversson & Machalski 2017	F127700
shark	Squatinidae	*Squatina* sp. indet.	Underwood 2004	F127702
dinosaur	Ornithopoda	Foot bones and fragments	Retallack *et al*. 2018	F127931
ichthyosaur	Opthalmosauridae	*Platypterygius americanus*	Merriam & Gilmore 1928	F127939
pterosaur	Dsungaripteridae	*Bennetazhia oregonensis*	Averianov 2012	Fig.7A-D

the local first appearance of *Mortoniceras inflatum* and below the local first appearance of *Mortoniceras fallax* (Fig.2), or 102.5–103.0 Ma (Lehmann 2015).

Material and methods

Excavation of the green breccia bed in the Hudspeth Formation northeast of Mitchell was active for 2 weeks in June 2021 with 82 volunteers from the North America Research Group, affiliated with the Rice Rock and Mineral Museum in Hillsboro, Oregon, and from the University of Oregon, in Eugene. A grid 6 by 10 m was laid out and the green breccia bed excavated in section (Fig. 3A) and in plan (Fig. 3B). Samples were collected for chemical analysis of major and trace elements by ALS Chemex of Vancouver, British Columbia (Table 2), by x-ray fluorescence (XRF) for

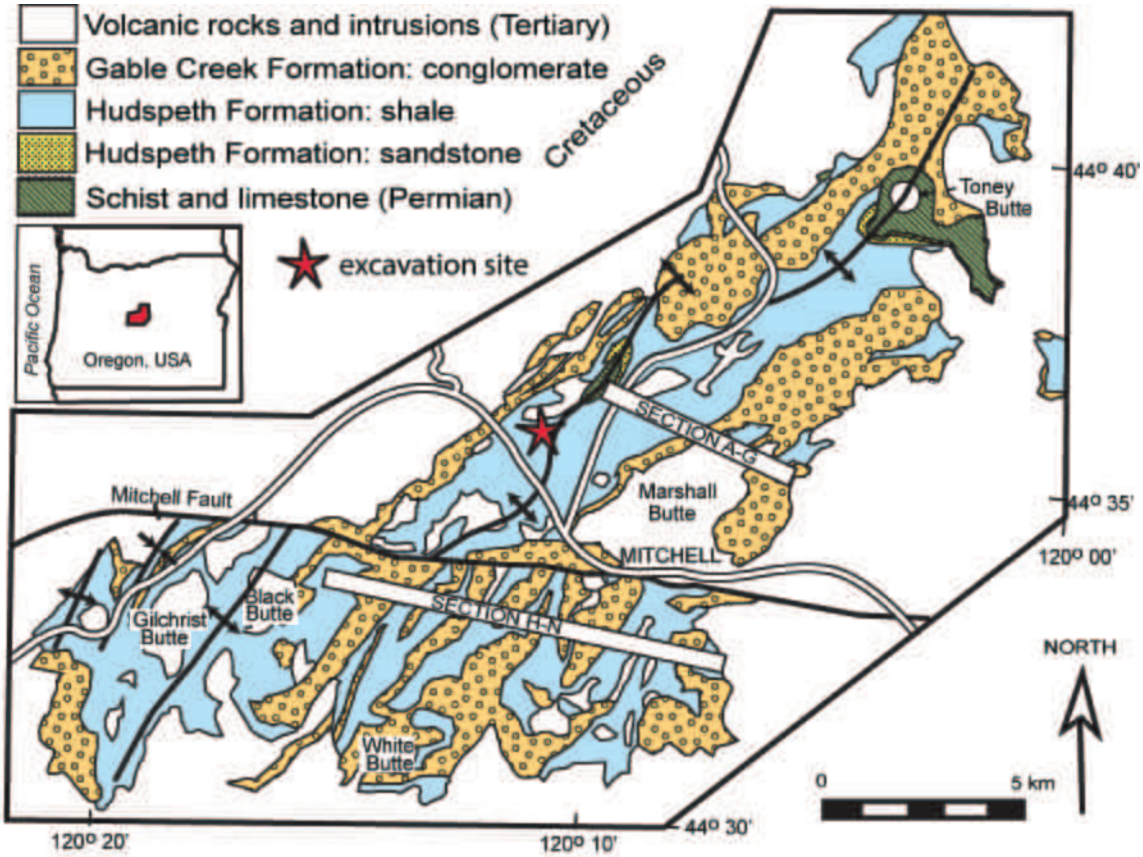

Fig. 1. Location of excavation near Mitchell, Wheeler County Oregon, and geological map of the Mitchell inlier (after Wilkinson & Oles 1968; Dorsey & Lenegan 2007).

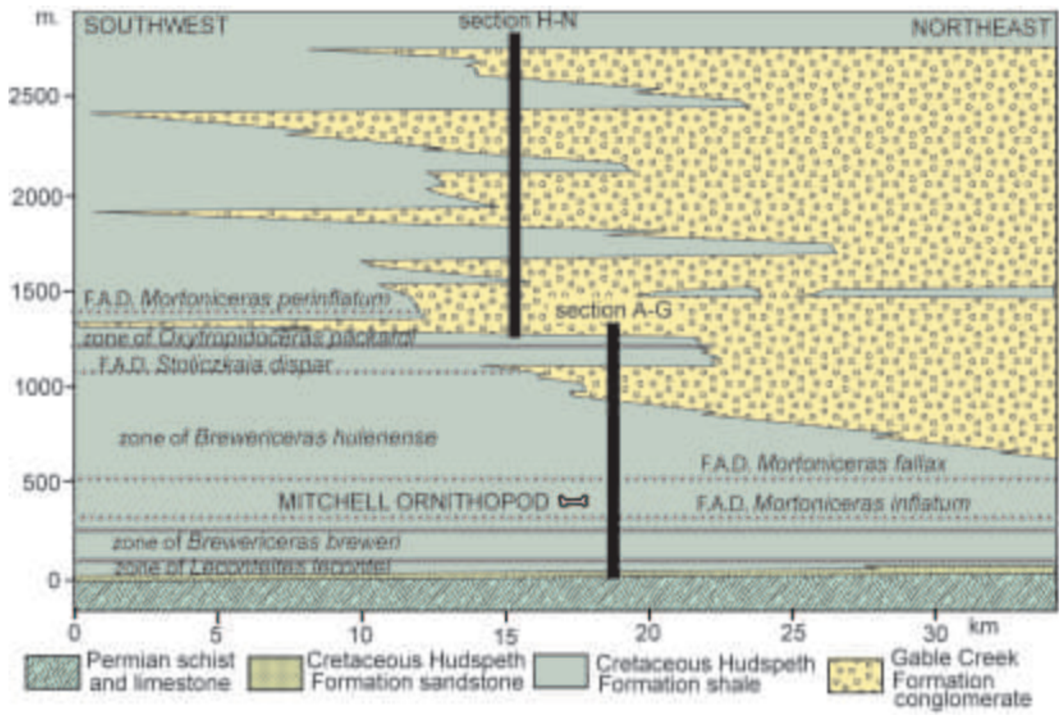

Fig. 2. Ammonite zones of the Hudspeth Formation in cross sections of Figure 2 (after Retallack *et al.* 2018).

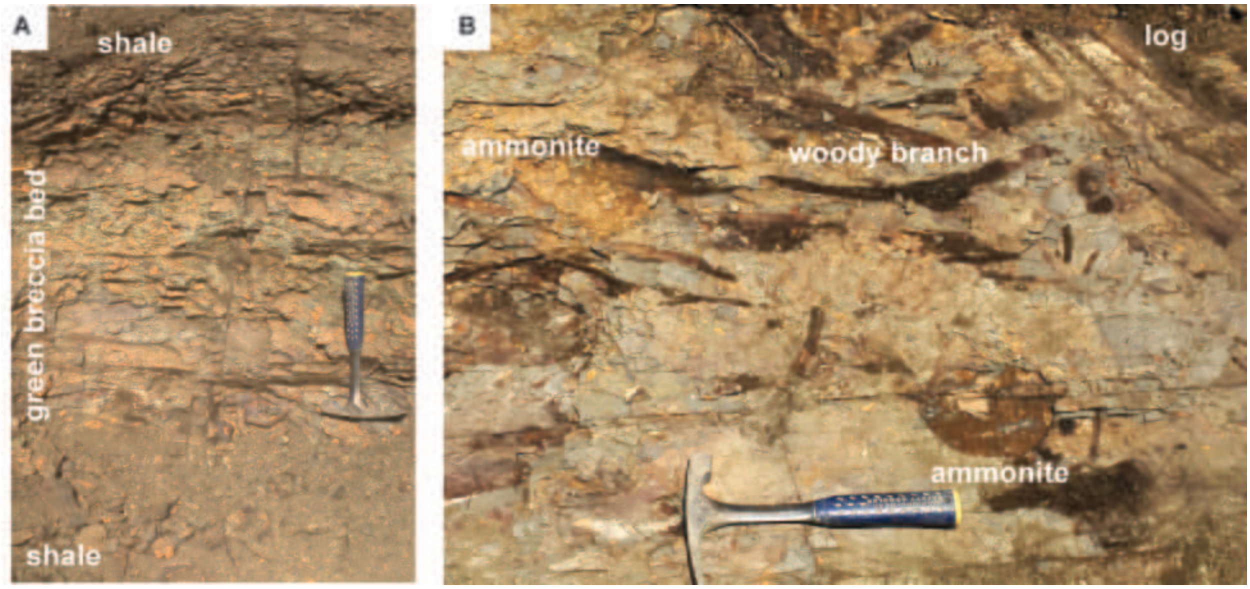

Fig. 3. Field photographs of (A) fossiliferous green breccia, and (B) excavated surface showing ammonites and woody debris. Scale for both is hammer with handle 25 cm long.

Table 2. Chemical analyses of the Hudspeth Formation

Lithology	Assay	shale	breccia	breccia	nodule	nodule	breccia	shale	
Level		0	20	30	40	75	55	90	
Sample #		R6396	R6397	R6398	R6399	R6400	R6401	R6402	error 1σ
SiO_2	wt %	55.4	56.1	57.3	21.8	58.6	27.1	55.6	2.705
Al_2O_3	wt %	15.95	14.95	15.7	6.7	15.35	7.23	16.55	0.825
T-Fe_2O_3	wt %	10.6	9	9.72	4.42	8.71	6.64	10.45	0.395
CaO	wt %	0.97	2.1	1.08	32.6	1.32	27.8	1.26	0.22
MgO	wt %	2.39	2.21	2.17	0.99	2.15	1.16	2.21	0.11
Na_2O	wt %	1.22	0.98	1.16	0.56	1.26	0.37	1.22	0.13
K_2O	wt %	1.86	2.44	2.47	1.08	2.01	1.08	2.01	0.025
Cr_2O_3	wt %	0.012	0.012	0.016	0.009	0.012	0.006	0.016	0.004
TiO_2	wt %	0.71	0.6	0.66	0.27	0.7	0.28	0.74	0.06
MnO	wt %	0.04	0.05	0.05	0.04	0.04	0.32	0.05	0.18
P_2O_5	wt %	0.17	0.37	0.24	22.6	0.48	1.1	0.19	0.03
SrO	wt %	0.01	0.01	0.01	0.11	0.01	0.03	0.01	0.02
BaO	wt %	0.05	0.04	0.06	0.04	0.06	0.03	0.06	0.03
LOI	wt %	9.77	10.35	10.1	6.99	9.06	26.1	10.75	0.35
Total	wt %	99.15	99.21	100.74	98.21	99.76	99.25	101.12	0.35
Ba	ppm	453	415	506	346	548	252	525	3.5
Ce	ppm	39.2	43.7	38.1	521	47.8	44.7	31.3	0.8
Cr	ppm	90	90	100	50	90	50	90	10
Cs	ppm	5.21	5.73	5.77	2.47	4.76	2.54	5.18	0.05
Dy	ppm	2.5	3.49	2.8	90.7	3.52	6.16	2.28	0.05
Er	ppm	1.83	2.05	1.91	44.1	2.31	3.18	1.67	0.03
Eu	ppm	0.61	1.1	0.8	27	0.96	1.73	0.49	0.02

Lithology	Assay	shale	breccia	breccia	nodule	nodule	breccia	shale	
Ga	ppm	18.1	23.8	22.7	12.7	17.7	11.6	17.4	0.1
Gd	ppm	2.58	4.1	3.01	101	3.55	6.27	2.09	0.05
Hf	ppm	3.3	3.2	3.1	1.4	3.7	1.7	3.3	0.1
Ho	ppm	0.52	0.72	0.55	16.55	0.79	1.11	0.44	0.01
La	ppm	18.8	18.6	17.3	205	23.6	20	15.8	0.4
Lu	ppm	0.34	0.3	0.29	2.75	0.38	0.31	0.26	0.01
Nb	ppm	7.2	6.5	6.2	2.9	8.1	3.1	6.9	0.1
Nd	ppm	16.6	21	17.4	268	18.7	22.7	13.5	0.3
Pr	ppm	4.26	5.14	4.4	57.2	5.19	5.23	3.55	0.07
Rb	ppm	67.7	96.6	90.3	41.9	73.5	41.6	68.1	0.2
Sm	ppm	3.02	4.59	3.32	77.6	3.78	5.57	2.28	0.06
Sn	ppm	2	2	2	2	2	1	2	1
Sr	ppm	99.4	103	87.5	943	110	233	96	3.5
Ta	ppm	0.6	0.5	0.4	0.2	0.6	0.2	0.5	0.1
Tb	ppm	0.39	0.56	0.46	14.3	0.56	0.94	0.31	0.01
Th	ppm	5.77	5.23	4.92	2.73	5.58	2.53	5.6	0.09
Tm	ppm	0.3	0.3	0.26	4.53	0.36	0.34	0.25	0.01
U	ppm	2.44	2.01	2.05	18.05	2.6	1.86	2.11	1
V	ppm	192	241	224	117	203	106	190	5
W	ppm	1	1	1	1	1	1	1	1
Y	ppm	13.9	18.7	14.8	633	22.3	36.2	12.1	0.3
Yb	ppm	1.95	2.03	2.11	22.8	2.62	2.08	2.03	0.03
Zr	ppm	116	117	111	52	125	53	111	2

major elements, and by inductively coupled plasma atomic emission spectrometry (ICP-AES) for rare earth elements. Total iron was determined as ferric, rather than ferrous. Site maps were made of the exposed upper surface of the green breccia, and fossils collected for conservation in the Condon Collection of the Museum of Natural and Cultural History of the University of Oregon. Sizes of whole ammonites, ammonite fragments and siderite-phosphate nodules were measured using digital calipers.

Description of the fossil bed

Facies and sedimentary structures

The green breccia bed is 50 cm thick, and is found throughout the 10-m-area of excavation within gray shales typical of this part of the Hudspeth Formation (Figs 3A). It dips 8° to the south east with a northeast strike azimuth of 033°. The breccia bed includes a 12-cm-thick graded bed at the base (Fig. 4), but the main part of the green breccia is crudely bedded to massive. It is a jumble of nodules, bones, teeth, ammonite fragments, and rounded pebbles of serpentinite, vein quartz, and sandstone, supported in a green clayey matrix. The green breccia contains common ellipsoidal siderite and phosphate nodules up to 5 cm in diameter and also a pervasive calcite cement. Scattered, rounded pebbles also up to 5 cm in diameter of quartz, granite, schist and greenstone were like those found in the interfingering Gable Creek Formation (Wilkinson & Oles 1968). Clasts in the main part of the green breccia are 65% small ammonite fragments, 10% bivalve fragments, 10% other fossil shell fragments, 7% igneous-metamorphic pebbles, 3% collophane nodules, 3% siderite nodules, and 2% bones and teeth. The uppermost part of the green breccia also contains large logs and branches of compressed conifer wood and scattered complete ammonites (Fig. 3). The orientation of woody debris was measured down the natural taper as a paleocurrent proxy, and the vector mean was toward the west, at azimuth 277° (Fig. 5).

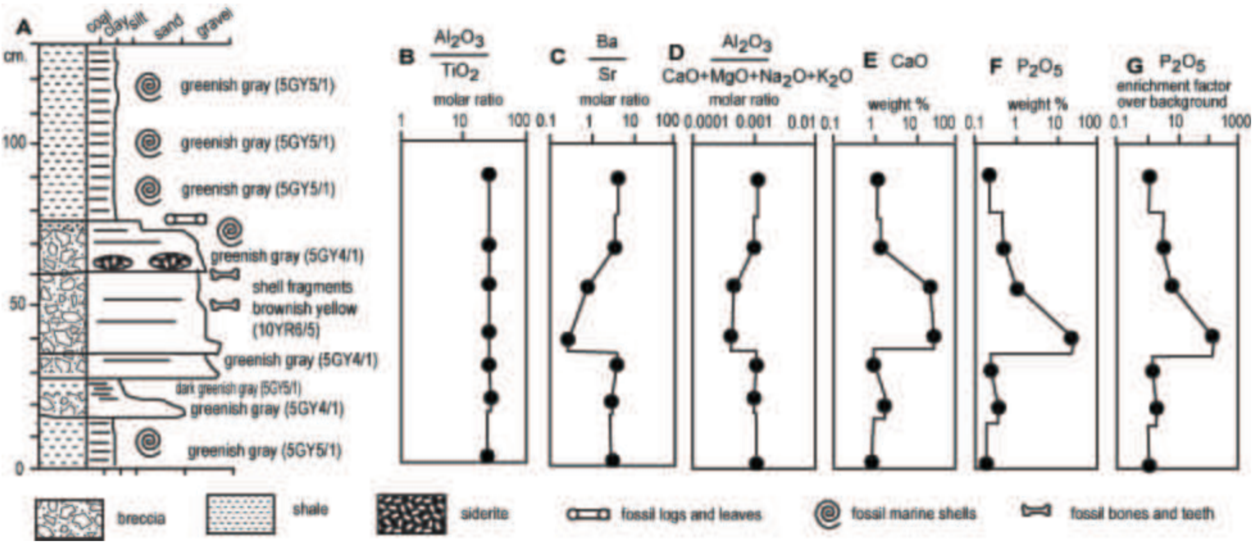

Fig. 4. Measured section of green breccia between grey shales, with selected molar weathering ratios and other geochemical measures.

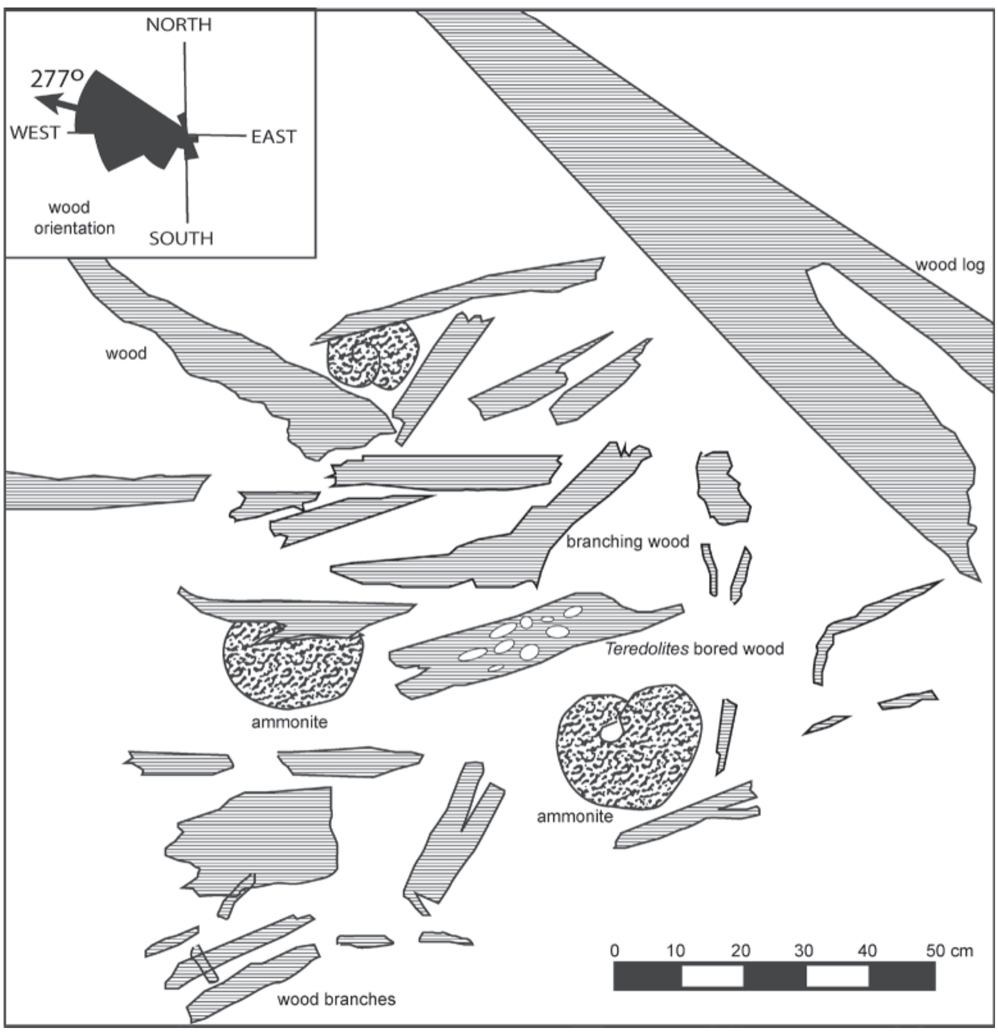

Fig. 5. Excavation plan and current rose for fossil logs for the upper green breccia northwest of Mitchell, Oregon.

Major element chemical composition

Molar ratios of alumina/titania are uniform throughout both the green breccia and shale above and below (Fig.4), reflecting common provenance. Both nodules analysed were ellipsoidal, very indurated, and fine-grained without bone or other inclusions, but one turned out to be siderite ($FeCO_3$) and the other turned out to be collophane ($Ca_5(PO_4)_3$). The collophane nodule was ellipsoidal without any external constrictions, or other markings of a coprolite. Phosphate was enriched in the green breccia compared with the shales above and below, and especially marked in the collophane nodule, but the siderite nodule had low phosphate like the shales (Fig. 4).

Rare earth element chemical composition

Rare earth spectra normalized to Post-Archaean Australian Shale of Taylor & McLennan (1985) are slightly enriched in heavy YREE and cluster together (Fig. 6). An exception is the collophane nodule (R6399), enriched in all YREE by almost two orders of magnitude. With depletions of both very heavy and very light REE the collophane nodule is not like marine (Hongo & Nozaki, 2001; Yasukawa *et al.* 2015) or non-marine rocks (Minařík *et al.* 1998; Munemoto *et al.* 2020). The siderite nodule (R6400), in contrast, shows a YREE array similar to shales and breccia. The ratio of light YREE, with atomic numbers 57–62, over heavy YREE, with atomic numbers 63–71, can be used to infer palaeoenvironment, and these values are shown in Figure 6. The light/heavy YREE ratios are mostly less than 3, as is typical for marine rocks (Hongo & Nozaki, 2001; Yasukawa *et al.* 2015). Much higher values of this ratio are found in soils and granites (Minařík *et al.* 1998; Munemoto *et al.* 2020). None of the YREE arrays show europium, cerium, or other anomalies indicative of hydrothermal alteration (Hongo & Nozaki 2001).

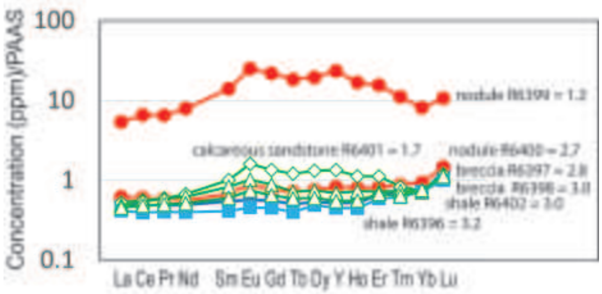

Fig. 6. YREE patterns normalized to Post-Archaean Australian Shale of the green breccia and contained nodules compared with shales of the Hudspeth Formation above and below.

Distribution of the fossils

Plants

Fossil plant compressions are not well preserved: no specimens had detachable cuticle, and wood was only partly permineralized in calcareous layers of the green breccia. A few trunks were limb casts entirely filled with non-carbonaceous, sparry calcite. All the fossil plants were broken (Fig. 9), and most were small fragments. One fossil log measured at 2.5 m long, but would have been from a much taller tree (Fig. 5). Its compressed width was 21 cm at 1.4 m above the base, and this can be taken as its original diameter, because lithostatic compaction crushes but does not spread fossil plants (Walton 1936). Using an allometric equation of Niklas (1994) for predicting tree height derived from diameter at breast height of 670 species of vascular plants gives an original predicted tree height of 5.4 ± 0.9 m (standard error of regression). This is not a large tree and may have been restricted in growth by onshore winds.

This new collection greatly increases the diversity of plant debris in the Hudspeth Formation, which was already known to include horsetails, ferns and conifers (Retallack *et al.* 2018). Notable is discovery of additional species of conifers and cycads (Table 1). The cycads are represented by numerous seeds, and some unusually coriaceous leaves (Fig. 9C-F). Comparison of the Hudspeth Formation flora with modern coast redwood vegetation of California (Retallack *et al.* 2018), can now be extended to include vegetation comparable with California coastal heath or chaparral (Barbour *et al.* 2007).

Marine invertebrates

This fossil site has been nicknamed the 'suture beds' because of common ammonite internal moulds. Of all the species present (Table 1), the most common is *Desmoceras alamoensis*, and these are preserved in an unusual way, with the upper half of the shell etched back to sutures, but the lower half of the external shell intact. The sutured upper surfaces of *D. alamoense* are seen in Figure 3B. The large specimen of *Mortoniceras inflatum* (Fig. 7E) was stabilized with Butvar (acetone solution of polyvinyl butyral resin), then undermined to collect for later preparation of the intact lower surface in the laboratory.

Invertebrate fossils found were marine species of ammonites, nautilids, snails, clams, regular urchins, and barnacles (Table 1). Pholad ('shipworm') bored wood (Fig. 5) and worn rounded edges of wood fragments are evidence that some of the wood was

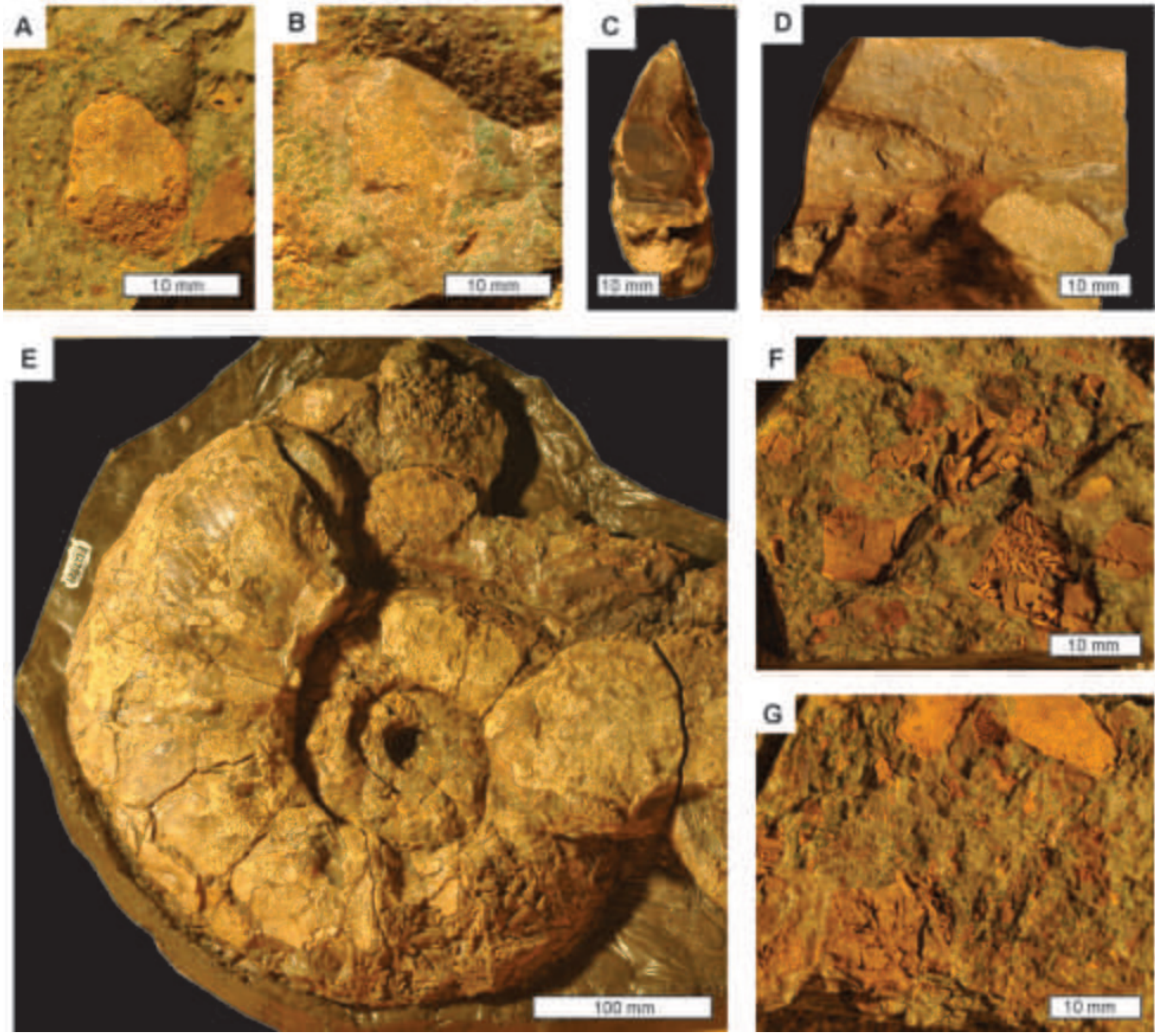

Fig. 7. Two teeth and lower mandible (cross section and side view) of pterosaur *Bennettazhia oregonensis* (A–D), complete ammonite *Mortoniceras inflatum* (E), and ammonite fragments (F, G). Specimen numbers are F127985A (A), F127910B (B), F127960 (C, D), F127929 (E), F12722D (F), F127922A (G).

marine driftwood. Especially notable are the many angular fragments of ammonites less than 2 cm in size, about the size of corn flake breakfast cereal, and a size range rare for intact ammonites in this deposit (Fig. 8). The modal diameter of whole ammonites in the deposit is 10 cm, with some up to 34 cm diameter, so that fragments are less than a fifth the size of whole shells. These fragments are highly angular and three dimensional with jagged edges of internal sutures still attached to portions of outer shell wall and so small they cannot be assigned to species. The ammonite fragmentation index (*F*) of Oloriz *et al*. (2004) uses the number of these highly fragmented, unidentifiable shells (*H*), as opposed to the number of sizeable pieces showing most of a whorl so identifiable (*M*),

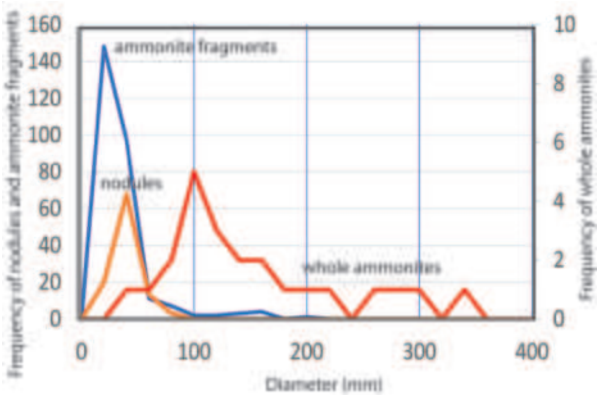

Fig. 8. Size distribution of ammonite fragments and nodules in the green breccia (on primary axis) compared with complete ammonite diameters (on secondary axis).

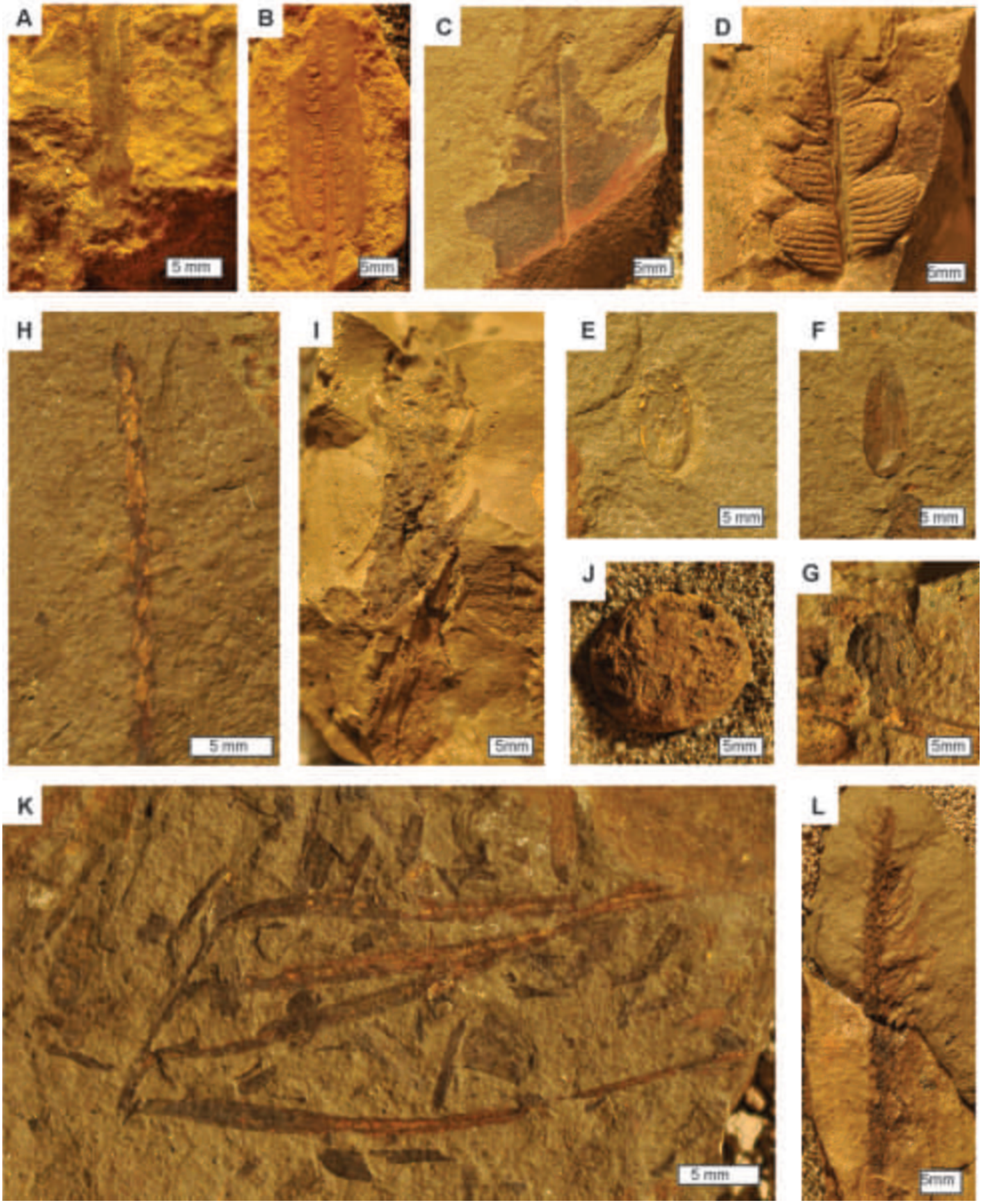

Fig. 9. Fossil plant impressions: horsetail *Equisetites burchardtii* (A), fern *Nathorstia angustifolia* (B), cycadeoid *Nilssonia canadensis* (C), cycadeoid *Nilssonia schaumbergensis* (D), *Cycadeospermum lineatum* (E-F), two seeded conifer cone unit (G), conifer shoot *Cyparissidium gracile* (H), conifer shoot and cone *Elatides splendida* (I, J), conifer shoot *Elatocladus smittiana* (K), conifer shoot *Margeriella cretacea* (L). Specimen numbers are F127880 (A), F120569 (B), F127957A (C), F127956 (D), F127982 (E), F127983E (F), F127961 (G), F127967 (H), F127963 (I), F127975 (J), F127072 (K), F127885A (L).

Fig. 10. The Oregon pterosaur *Bennettazhia oregonensis*, with 4-m-wingspan, reconstructed independently in seagull colours by Midiaou Diallo, and reproduced with permission.

and number of shells with the margin reconstructable (*L*), as in equation 1.

$$F = \frac{(100H + 50M + 1L)}{(H + M + L)}$$

By this metric the green breccia has an ammonite fragmentation index of 89.1% of 297 measured specimens, an exceptional degree of fragmentation compared with this same metric for ammonites in a variety of nearshore to offshore limestones and shale of 25–70% (Oloriz *et al.* 2004). This degree of fragmentation is the most extreme in our combined experience of ammonite fossil localities, also unparalleled in modern *Nautilus* shells on beaches and reefs (Mapes *et al.* 2010; Hembree *et al.* 2014).

Vertebrates

Fragmentary bones and teeth are dispersed within the green breccia (Fig. 7A-B). These include fragments of dinosaurs, comparable with the unidentified, large (estimated 5 m long) ornithopod found at another locality nearby (Retallack *et al.* 2018). Also found were fragments of bony fish, sharks, ichthyosaurs, and pterosaurs (Table 1). Remains of ichthyosaurs from Mitchell are fragmentary (Merriam & Gilmore 1928), and probably represent *Platypterygius americanus* (McGowan 1972; Maxwell & Kear 2010). None of the vertebrates were found articulated, or with fresh breaks. Nor do they show rounding, nor size sorting within the green breccia.

Interpretations

Tempestite coquina

Large storms and declining sedimentation rates of hardgrounds have the effect of winnowing shells from mud and silts, and concentrating them into thick, clast-supported, coquinas on beaches or shallow marine shelves (Kidwell 1985), as documented mainly for bivalves (Williams 2011), but also for modern *Nautilus* shells which can be considered comparable with ammonite assemblages (Hembree *et al.* 2014). Storm concentrations leave most shells intact, though many shells have borings and encrustations from prior exposure (Wilson 2007; Suess *et al.* 2016). Tempestites also include shells with worn and rounded edges from surf and beach abrasion (Pilkey *et al.* 1967; Leighton *et al.* 2016; Kwarteng *et al.* 2016). Despite common plant debris, the green breccia has no root traces, so was not a paleosol or deposited on a paleosol (Retallack & Dilcher, 2012). Nor are there dune, nor shoreface sedimentary structures such a cross bedding, nor parting lineation (Reineck & Singh, 2012), as evidence of a beach or coastal dune setting. Rarity of borings and encrustations in sharp uncorroded ammonite fragments that are matrix supported, distinguishes the green breccia near Mitchell from tempestite or other marine coquinas. The green breccia bed appears to be an event deposit with sharp erosional base, unrelated to sea level change, and with no indications of marine hardground cementation or hard substrate molluscs such as encrusting oysters.

Submarine paleoenvironment for the green breccia is also in evidence from preservation in its upper part of ammonite shells thoroughly dissolved on the upper side, but intact on the lower side (Fig. 7E), as is well known in marine shales (Maeda 1987), and ammonitico rosso limestones (Jenkyns 1974; Bosellini *et al.* 1975). In pelagic limestones of the ammonitico rosso, dissolution was related to subsidence of the seafloor or rise in oceanic carbonate compensation depth (CCD) within the deep sea (Bosellini *et al.* 1975). Nodular Cretaceous marine shales of the Yezo Formation of Japan are like the Hudspeth Formation in showing shale infill of ammonite upper surfaces dissolved on, or at shallow depths within, seafloor muds (Maeda 1987). Dissolution may have been due to acidic, fresh, storm water in shallow shelf environments, but also likely for the Hudspeth Formation is dissolution of the upper surface of beached ammonite shells carried back into the ocean with associated plant debris by debris flow. The green breccia does not appear to have been a deposit of storms or other winnowing of shells under water or on the seashore.

Tsunamite

Tsunamis are not necessarily large waves breaking on shore, but begin with rising water that does not erode the bed, and only subsequently inflates to sweep most objects in its path inland (Szczuciński *et al*. 2012). The salient features of tsunamites are offshore sand carried inland with a variety of debris, without significant erosion of the basal bed, and yet only 10–20 cm thick (Atwater *et al*. 1992; Atwater and Hemphill-Haley 1997; Cisternas *et al*. 2005).

Tsunamites are a poor match for the green breccia, which does appear to have an erosional base, is much thicker than known tsunamites, and has abundant pebbles and plant debris transported seaward rather than inland.

Regurgitalite

The unusually thorough fragmentation of ammonites in the green breccia bed (Fig. 8) is a hallmark of durophagous predators (Zuschin *et al.* 2003), either as regurgitalites (Hoffmann *et al*. 2019), or as a midden (discussed in the next section). Debris flows commonly preserve unweathered, entire shells and bones, and are not capable of extreme fragmentation (Wendt & Aigner 1985; Keefer *et al.* 2003; Nelson *et al.* 2009). Nor can storms or exposure fragment modern *Nautilus* to the extent seen in the green breccia (Wani 2004; Mapes *et al*. 2010; Hembree *et al.* 2014). Regurgitated fragments of shells are relatively uniform in size (2–3 cm), corroded and rounded by stomach acid, and with a distinct preference for calcitic aptychi rather than aragonitic shell fragments (Sato & Tanabe 1998; Hoffmann *et al.* 2019). They also are clustered in thin (1–2 cm) patches less than a metre in diameter within marine shales (Zatoń & Salamon 2008). Different regurgitalites reveal dietary preferences: ammonites for coleoid squid, sharks, fish and plesiosaurs (Sato & Tanabe 1998; Zatoń & Salamon 2008; Hoffmann *et al.* 2019), fish for Rhamphorynchid, Wukongopterid and Anhanguerian pterosaurs (Jiang *et al*. 2022), and squid, belemnites, and fish for ichthyosaurs (Massare & Young 2005).

Regurgitalites are a poor match for the green breccia, which extends throughout our excavation with a thickness of 60 cm (Figs 3, 4), and is full of small (1–2 cm), uncorroded ammonite shell fragments (Fig. 7F–G) as well as plant debris including tree trunks (Fig. 5).

Debris flow of guano midden

The green breccia has sedimentary structures and textures of a debris flow deposit: massive, matrix supported gravel and larger clasts within a clayey matrix (Hubert & Filipov 1989; Chen *et al*. 2008). If the large woody debris near the top is included, the deposit could be regarded as inverse graded, perhaps by a mechanism of kinetic sieving (Middleton 1970), widely known in debris flows (Naylor 1980). More likely, the large woody debris and entrained ammonite shells (Fig. 5) floated above the debris flow when it hit the water. Debris flows are found in mountain foothills (Bardou *et al.* 2007) to deep sea (Embley 1976), but the green breccia debris flow of the Hudspeth Formation was neither. It was lodged within a shallow marine shale as indicated by the high proportion of plant material including tree trunks, and marine fauna of flat clams and regular urchins (Table 1). The siderite nodule (R6400) was derived by erosion of shale, and is similar to nodules at other stratigraphical levels in the Hudspeth Formation. Preservation of dinosaur and other remains in a debris flow is an alternative to the float and bloat model for deposition of isolated dinosaur remains in marine rocks, suggested by Peecook & Sidor (2015) and Retallack *et al.* (2018).

The collophane nodule (R6399) was derived from a YREE source unlike any of the other rocks analysed (Fig.6), although its aluminosilicates were similar (Fig. 4). The phosphorus-rich composition of the green breccia (Fig. 4), suggests that the source may have included guano. Thick deposits of guano from sea birds on Pacific islands remain an important source of agricultural fertilizer, but their accumulation within karst depressions of dolomitized limestone (Power 1925; Piper *et al.* 1986; Morrison & Manner, 2005) is unlike the Cretaceous coast of non-calcareous schists with only narrow metamorphosed lenses of fusulinid limestone in central Oregon (Wilkinson & Oles 1958). A better modern analog is guano and phosphorites off the coast of Chile and Peru, which include both thick accumulations of subaerial guano, as well as apatite nodules in shallow marine shales (Burnett 1977; Burnett & Veeh, 1977; Burnett & Lee 1980). Dongdao Island in the South China Sea has Pleistocene coastal terraces with alternating beds of marine marl and guano-enriched debris flows related to sea level change (Liu *et al.* 2008). The phosphatic green clay matrix to the green breccia may be from the debris flow entraining guano that catastrophically included tree trunks, sea shells and bones. The mechanical qualities of bat guano are comparable with those of clay, and form debris flows if water saturated or agitated seismically (Dykes 2007). Earthquake initiation of the debris flow is plausible, because at that time the Hudspeth Formation was deposited in a forearc basin (Surpless & Gulliver 2018).

Most similar to the Hudspeth Formation mollusc fragments in size range and angularity, are bivalve fragments in middens produced by dropping onto rocks and pecking by herring gulls (Cadée 1995). Thus the source of abundant shell fragments in the green breccia may have been a midden of a durophagous predator onshore. The land was also the source of igneous-metamorphic pebbles, collophane nodules, bones and teeth of dinosaurs and pterosaurs, and a variety of wood and other plant fragments. Other components appear marine, and would have been entrained during debris flow emplacement in the ocean, including siderite nodules, identifiable ammonite shells, collophane nodules and ichthyosaur, fish and shark bones and teeth.

With regard to the organisms fragmenting shells in the Hudspeth Formation, birds are unlikely because gastroliths of early Cretaceous birds are evidence of herbivory rather than mollusc-eating (Chiappe *et al.* 2014; O'Connor *et al.* 2018). Analysing the fossil record of Cretaceous birds from China, Mitchell *et al.* (2014) conclude that, 'The Jehol avifauna has few representatives of highly preservable ecomorphs (e.g. aquatic forms) and a notable lack of ecomorphological overlap with the pterosaur assemblage (e.g. no large or aerially foraging pygostylians). Comparisons of the Jehol functional diversity with modern and subfossil avian assemblages show that taphonomic bias alone cannot explain the ecomorphological impoverishment.' Bivalve consumption by humans (Faulkner 2013), fish (Cate & Evans 1994), crabs (Elner 1978), and starfish (Carter 1968) results in chipping around the edges or a few big pieces, unlike the thorough comminution of ammonites seen in the green breccia bed (Fig. 8).

A more likely durophagous predator for the green breccia ammonite fragments is the pterosaur *Bennettazhia oregonensis*, named by Nesov (1991) from an undeformed humerus and vertebrae first reported by Gilmore (1928) from a roadcut southwest of Mitchell at a higher stratigraphical level within the Hudspeth Formation than the green breccia (2121 m in Fig. 2). The humerus has internal trabeculae, but thin outer wall indicating that it was related to azhdarchids (Habib 2007), as proposed by Bennett (1989) and Nesov (1991). Bennett (1994) later compared *Bennetazhia* with *Dsungaripterus*. The cladogram of Andres *et al.* (2014) has *Bennettazhia* as an azhdarchoid basal within the clade Tapejaromorpha, including *Tapejara*, and independent from Neoazhdarchia including *Dsungaripterus*. A recent cladogram of Andres (2021) does not include *Bennetazhia* for reasons of incomplete data, but supporting text does not alter the conclusion of Andres *et al.* (2014).

Pterosaur remains found in our excavation include isolated teeth (Fig. 7A, B), and an edentulous section of mandible with very dense bone (Fig. 7C, D). *Dsungaripterus* had a hard edentulous outer rostrum, with lateral grooves that may have been the basal attachment of a chitinous beak (Chen *et al.* 2020), similar to grooves in the new Oregon material (Fig. 7C-D). '*Dsungaripterus* might have picked out bivalves, gastropods and crabs with its jaw tips before cracking open their shells or exoskeletons with its teeth' (Bestwick *et al.* 2018). Similarly in *Tapejara*, 'The toothless beak is slender and pointed, and seems best adapted for plucking or picking. Therefore, a frugivorous feeding habit is suggested' (Wellnhofer 1991). Duriphagous predation by *Bennettazhia* inferred here would be a specialization over obligate piscivory inferred for Jurassic pterosaurs *Rhamphorychus*, *Kunpenopterus*, and *Guidraco* (Jiang *et al.* 2022), and flamingo-like cyanobacterial filter-feeding inferred for Early Cretaceous *Pterodaustro* (Codorniú *et al.* 2013).

Conclusions

An enigmatic green breccia bed with tree trunks and other plant fragments, pebbles and nodules, marine bivalves and snails, ammonite shells and fragments, defies usual pH-Eh controls of fossil preservation (Retallack 1984). It is interpreted as an event deposit, or more specifically a debris flow from the land out into the shallow sea. The high phosphorus content of the green breccia suggests that it included guano (Burnett & Lee 1980; Jiang *et al.* 2022). Abundant, finely comminuted ammonite shell fragments are like those of middens of mollusc-eaters like modern herring gulls (Cadée 1995), but comparable diet and behavior is unknown and unlikely in Early Cretaceous birds (Mitchell *et al.* 2014). The hard edentulous outer rostrum of Early Cretaceous azhdarchid pterosaurs, such as Oregon's *Bennetazhia oregonensis* (Nesov 1991) has been proposed as an adaptation to mollusc feeding (Wellnhofer 1991; Bestwick *et al.* 2018). The green breccia may thus represent a debris flow into the shallow sea from coastal guano and midden deposits of Early Cretaceous (Albian) pterosaurs.

Acknowledgments. – We thank Ryan Griffin, Erin Woodard and Lenore Heppler of the Bureau of Land Management for excavation permit 51066. For help with collecting we especially thank Christine Broz, Rana Gahwagy, Tara Baker, Aaron Currier, Andrew Bland, and Richard Bland. Peter Rodda helped enormously with ammonite identifications. Also helpful were discussions with David Jones, Rebecca Dorsey, Nathan Sheldon, Bill Orr, David Taylor, and John Dilles.

References

Andres, B., Clark, J. & Xu, X. 2014: The earliest pterodactyloid and the origin of the group. *Current Biology 24*, 1011–1016.

Anderson, F.M. 1938: Lower Cretaceous Deposits in California and Oregon. *Geological Society of America Special Paper 16*, 1–339.

Anderson, F.M. 1958: Upper Cretaceous of the Pacific coast. *Geological Society of America Memoir 71*, 1–378.

Andres, B. 2021: Phylogenetic systematics of *Quetzalcoatlus* Lawson 1975 (Pterodactyloidea: Azhdarchoidea). *Journal of Vertebrate Paleontology 41, supplement 1*, 203–217.

Atwater, B.F. & Hemphill-Haley, E. 1997: Recurrence intervals for great earthquakes of the past 3500 years at northeastern Willapa Bay, Washington. *U.S. Geological Survey Professional Paper 1576*, 1–108.

Atwater, B.F., Núñez, H.J. & Vita-Finzi, C. 1992. New late Holocene emergence despite earthquake-induced submergence, south-central Chile. *Quaternary International 15–16*, 77–85.

Barbour, M.G., Keeler-Wolf, T. & Schoenherr, A.A. 2007: *Terrestrial Vegetation of California*. University of California Press, Berkeley.

Bardou, E., Boivin, P., & Pfeifer, H.R., 2007: Properties of debris flow deposits and source materials compared: implications for debris flow characterization. *Sedimentology 54*, 469–480.

Barthel, K.W., Swinburne, N.H.M. & Morris, S.C. 1990: *Solnhofen: A Study in Mesozoic Palaeontology*. Cambridge University Press, Cambridge, 245 p.

Baumgartner, A. & Peppe, D.J. 2021: Paleoenvironmental changes in the Hiwegi Formation (lower Miocene) of Rusinga Island, Lake Victoria, Kenya. *Palaeogeography Palaeoclimatology Palaeoecology 574*, 110458.

Bell, W.A. 1956: Lower Cretaceous floras of western Canada. *Geological Survey of Canada Memoir 285*, 1–331.

Bennett S.C. 1989: Pathologies of the large pterodactyloid pterosaurs *Ornithocheirus* and *Pteranodon*. *Journal of Vertebrate Paleontology 9*, 13A.

Bennett S.C. 1994: Taxonomy and systematics of the Late Cretaceous pterosaur *Pteranodon* (Pterosauria, Pterodactyloidea). *Occasional Paper Natural History Museum University of Kansas 169*, 1–170

Berry, E.W. 1922: The flora of the Cheyenne Sandstone of Kansas. *U.S. Geological Survey Professional Paper 129I*, 199–231.

Bestwick, J., Unwin, D.M., Butler, R.J., Henderson, D.M. & Purnell, M.A. 2018: Pterosaur dietary hypotheses: a review of ideas and approaches. *Biological Reviews 93*, 2021–2048.

Bosellini, A. & Winterer, E.L. 1975: Pelagic limestone and radiolarite of the Tethyan Mesozoic: a genetic model. *Geology 3*, 279–282.

Bromley, R.G., Pemberton, S.G. & Rahmani, R.A. 1984: A Cretaceous woodground: the *Teredolites* ichnofacies. *Journal of Paleontology 58*, 488–498.

Burnett, W.C. 1977: Geochemistry and origin of phosphorite deposits from off Peru and Chile. *Geological Society of America Bulletin 88*, 813–823.

Burnett, W.C. & Lee, A.I.N. 1980: The phosphate supply system in the Pacific region. *GeoJournal 4*, 423–435.

Burnett, W.C. & Veeh, H.H. 1977: Uranium-series disequilibrium studies in phosphorite nodules from the west coast of South America. *Geochimica et Cosmochimica Acta 41*, 755–764.

Cadée, G.C. 1995: Birds as producers of shell fragments in the Wadden Sea, in particular the role of the Herring gull. *Geobios 18*, 77–85.

Carter, R.M. 1968: On the biology and palaeontology of some predators of bivalved Mollusca. *Palaeogeography, Palaeoclimatology, Palaeoecology 4*, 29–65.

Cate, A.S. & Evans, I. 1994: Taphonomic significance of the biomechanical fragmentation of live molluscan shell material by a bottom-feeding fish (*Pogonias cromis*) in Texas coastal bays. *Palaios 9*, 254–274.

Chiappe, L.M., Zhao, B., O'Connor, J.K., Chunling, G., Wang, X., Habib, M., Marugan-Lobon, J., Meng, Q. & Cheng, X. 2014: A new specimen of the Early Cretaceous bird *Hongshanornis longicresta*: insights into the aerodynamics and diet of a basal ornithuromorph. *PeerJ 2*, e234.

Chen, J., Dai, F., & Yao, X., 2008. Holocene debris-flow deposits and their implications on the climate in the upper Jinsha River valley, China. *Geomorphology 93*, 493–500.

Chen, H., Jiang, S., Kellner, A.W., Cheng, X., Zhang, X., Qiu, R., Li, Y. & Wang, X. 2020: New anatomical information on *Dsungaripterus weii* Young, 1964 with focus on the palatal region. *PeerJ 8*, e8741.

Cisternas, M., Atwater, B.F., Torrejón, F., Sawai, Y., Machuca, G., Lagos, M., Eipert, A., Youlton, C., Salgado, I., Kamataki, T., Shishikura, M., Rajendran, C.P., Malik, J.K., Rizal, Y. & Husni, M. 2005: Predecessors of the giant 1960 Chile earthquake. *Nature 437*, 404–407.

Clark, D.L. 1965: Heteromorph ammonoids from the Albian and Cenomanian of Texas and adjacent areas. *Geological Society of America Memoir 95*, 1–99.

Codorniú, L., Chiappe, L.M. & Cid, F.D. 2013: First occurrence of stomach stones in pterosaurs. *Journal of Vertebrate Paleontology 33*, 647–654.

Dorsey, R.J. & Lenegan, R.J. 2007: Structural controls on middle Cretaceous sedimentation in the Toney Butte area of the Mitchell inlier, Ochoco basin, central Oregon. In Cloos, M., Carlson, W.D., Gilbert, M.C., Liou, J.G., & Sorensen, S.S. (eds), Convergent Margin Terranes and Associated Regions: A Tribute to W.G. Ernst. *Geological Society of America Special Paper 419*, 97–126.

Dykes, A.P. 2007: Mass movements in cave sediments: investigation of a~ 40,000-year-old guano mudflow inside the entrance of the Great Cave of Niah, Sarawak, Borneo. *Landslides 4*, 279–290.

Elner, R.W. 1978: The Mechanics of Predation by the Shore Crab, *Carcinus maenas* (L.), on the Edible Mussel, *Mytilus edulis* L. *Oecologia 36*, 333–344.

Embley, R.W. 1976: New evidence for occurrence of debris flow deposits in the deep sea. *Geology 4*, 371–374.

Etter, W. & Tang, C.M. 2002: Posidonia Shale: Germany's Jurassic marine park. In Bottjer, D.J., Etter, W., Hagadorn, J.W. & Tang, C.M. (eds), *Exceptional fossil preservation*. Columbia University Press, New York, p. 265–291.

Faulkner, P., 2013: *Life on the Margins: An Archaeological Investigation of Late Holocene Economic Variability, Blue Mud Bay, Northern Australia*. Australian National University Press, Canberra, 216 p.

Frigo, M. & Sorbini, C. 1999: *Fossili di Bolca*. Electa, Verona.

Gautam, J.P., Pandey, B., Jaitly, A.K., Pathak, D.B., Lehmann, J. & Tiwari, D.N. 2019: Late Albian ammonites from the Cauvery Basin, south India. *Cretaceous Research 102*, 12–29.

Gilmore, C.W. 1928: A new pterosaurian reptile from the marine Cretaceous of Oregon. *United States National Museum Proceedings 73*, 1–5.

Habib, M. 2007: Structural characteristics of the humerus of *Bennettazhia oregonensis* and their implications for specimen diagnosis and azhdarchoid biomechanics: *Flugsaurier: Abstracts of the Wellnhofer pterosaur meeting, Bavarian State Collection for Palaeontology, Munich, 1*, 16.

Hembree, D.I., Mapes, R.H. & Goiran, C. 2014: The impact of high-energy storms on shallow-water Nautilus (Cephalopoda) taphonomy, Lifou (Loyalty Islands). *Palaios 29*, 348–362.

Hoffmann, R., Stevens, K., Keupp, H., Simonsen, S. & Schweigert, G. 2020: Regurgitalites–a window into the trophic ecology of fossil cephalopods. *Journal of the Geological Society, 177*, 82–102.

Hongo, Y. & Nozaki, Y. 2001: Rare earth element geochemistry of hydrothermal deposits and *Calyptogena* shell from the Iheya Ridge vent field, Okinawa Trough. *Geochemical Journal 35*, 347–354.

Housen, B.A. & Dorsey, R.J. 2005: Paleomagnetism and tectonic significance of Albian and Cenomanian turbidites, Ochoco basin, Mitchell Inlier, central Oregon. *Journal of Geophysical Research, Solid Earth 110*, B07102.

Hubert, J.F. & Filipov, A.J. 1989: Debris-flow deposits in alluvial fans on the west flank of the White Mountains, Owens Valley, California, USA. *Sedimentary Geology 61*, 177–205.

Imlay, R.W. 1961. Characteristic lower Cretaceous megafossils from northern Alaska. *U.S. Geological Survey Professional Paper 335*, 1–74.

Jashemski, W.M.F. & Meyer, F.G. 2002: *The natural history of Pompeii*. Cambridge University Press, Cambridge, 528 p.

Jenkyns, H.C. 1974: Origin of red nodular limestones (Ammonitico Rosso, Knollenkalke) in the Mediterranean Jurassic: a diagenetic model. *In* Hsü, K.J., & Jenkyns, H.C. (eds), *Pelagic Sediments: On Land and Under the Sea*. John Wiley, Chichester, p. 249–271.

Jiang, S., Wang, X., Zheng, X., Cheng, X., Wang, X., Wei, G. & Kellner, A.W. 2022: Two emetolite-pterosaur associations from the Late Jurassic of China: showing the first evidence for antiperistalsis in pterosaurs. *Philosophical Transactions of the Royal Society B377*, 20210043.

Jones, D.L. 1960: Lower Cretaceous (Albian) fossils from South-Western Oregon and their paleogeographic significance. *Journal of Paleontology 34*, 152–160.

Jones, D.L., Murphy, M.A. & Packard, E.L. 1965: The Lower Cretaceous (Albian) ammonite genera *Leconteites* and *Brewericeras*. *U.S. Geological Survey Professional Paper 503-F*, 1–21.

Kawabe, F. & Haggart, J.W. 2003: The ammonoid *Desmoceras* in the Upper Albian (Lower Cretaceous) of Japan. *Journal of Paleontology 77*, 314–322.

Keefer, D.K., Moseley, M.E. & Defrance, S.D. 2003: A 38 000-year record of floods and debris flows in the Ilo region of southern Peru and its relation to El Niño events and great earthquakes. *Palaeogeography, Palaeoclimatology, Palaeoecology 194*, 41–77.

Kidwell, S.M. 1985: Palaeobiological and sedimentological implications of fossil concentrations. *Nature 318*, 457–460.

Kvaček, J. & Dašková, J. 2007: Revision of the type material in the genus *Nathorstia* Heer (Filicales). *Journal of the National Museum Prague Natural History Series 176*, 117–123.

Kwarteng, A.Y., Al-Hatrushi, S.M., Illenberger, W.K. & McLachlan, A. 2016: Grain size and mineralogy of Al Batinah beach sediments, Sultanate of Oman. *Arabian Journal of Geosciences 9*, 1–18.

Kleinhans, L.C., Balcells-Baldwin, E.A. & Jones, R.E. 1984: A paleogeographic reinterpretation of some middle Cretaceous units, north-central Oregon: evidence for a submarine turbidite system. In Nilsen, T.H. (ed.), *Geology of the upper Cretaceous Hornbrook Formation, Oregon and California*. Pacific Section Society of Economic Paleontologists and Mineralogists, Los Angeles, 239–257.

Lehman, J. 2015: Ammonite biostratigraphy of the Cretaceous—an overview. In Klug, C., Korn, D., De Baets, K., Kruta, I., & Mapes, R.H. (eds), *Ammonoid Paleobiology: From macroevolution to paleogeography*. Springer, Dordrecht, 403–429.

Leighton, L.R., Chojnacki, N.C., Stafford, E.S., Tyler, C.L. & Schneider, C.L. 2016: Categorization of shell fragments provides a proxy for environmental energy and predation intensity. *Journal of the Geological Society of London 173*, 711–715.

Liu, X.D., Sun, L.G., Cheng, Z.Q., Zhao, S.P., Liu, K.X., Wu, X.H., Xie, Z.Q., Yin, X.B., Luo, H.H., Ding, X.F. & Fu, D.B. 2008: Paleoenvironmental implications of the guano phosphatic cementation on Dongdao Island in the South China Sea. *Marine Geology, 247*, 1–16.

Maeda, H. 1987: Taphonomy of ammonites from the Cretaceous Yezo Group in the Tappu area, northwestern Hokkaido, Japan. *Paleontological Society of Japan Transactions Proceedings 148*, 285–305.

Mapes, R.H., Landman, N.H., Cochran, K., Goiran, C., de Forges, B.R. & Renfro, A. 2010: Early taphonomy and significance of naturally submerged *Nautilus* shells from the New Caledonia region. *Palaios 25*, 597–610. https://doi.org/10.2110/palo.2009.p09-109r

Massare, J.A. & Young, H.A. 2005: Gastric contents of an ichthyosaur from the Sundance Formation (Jurassic) of central Wyoming. *Paludicola 5*, 20–27.

Maxwell, E.E. & Kear, B.P. 2010: Postcranial anatomy of *Platypterygius americanus* (Reptilia: Ichthyosauria) from the Cretaceous of Wyoming. *Journal of Vertebrate Paleontology 30*, 1059–1068.

Merriam, J.C. & Gilmore, C.W. 1928: An ichthyosaurian reptile from the marine Cretaceous of Oregon. *Carnegie Institution of Washington Publication 393*, 3–4.

Middleton, G.V. 1970: Experimental studies related to problems of flysch sedimentation. In Lajoie, J. (ed.), Flysch Sedimentology in North America. *Geological Association of Canada Special Paper 7*, 253–272.

Miller, C.N. & LaPasha, C.A. 1984: Flora of the Early Cretaceous Kootenai Formation in Montana, conifers. *Palaeontographica B193*, 1–17.

Minařík, L., Žigová, A., Bendl, J., Skřivan, P. & Šťastnýd, M. 1998: The behaviour of rare-earth elements and Y during the rock weathering and soil formation in the Říčany granite massif, Central Bohemia. *Science of the Total Environment 215*, 101–111.

Mitchell, J.S. & Makovicky, P.J. 2014: Low ecological disparity in Early Cretaceous birds. *Proceedings Royal Society of London B281*, 20140608

Morrison, R.J. & Manner, H.I. 2005: Pre-mining pattern of soils on Nauru, central Pacific. *Pacific Science 59*, 523–540.

Munemoto, T., Solongo, T., Okuyama, A., Fukushi, K., Yunden, A., Batbold, T., Altansukh, O., Takahashi, Y., Iwai, H. & Nagao, S. 2020: Rare earth element distributions in rivers and sediments from the Erdenet Cu–Mo mining area, Mongolia. *Applied Geochemistry 123*, 104800

McGowan, C. 1972: The systematics of Cretaceous ichthyosaurs with particular reference to the material from North America. *Rocky Mountain Geology 11*, 9–29.

Murphy, M.A. 1967: Aptian-Cenomanian members of the ammonite genus *Tetragonites*. *University of California Publications in Geological Sciences 69*, 1–79.

Naylor, M.A. 1980: The origin of inverse grading in muddy debris flow deposits; a review. *Journal of Sedimentary Research 50*, 1111–1116.

Nelson, A.E., Smellie, J.L., Hambrey, M.J., Williams, M., Vautravers, M., Salzmann, U., McArthur, J.M. & Regelous, M. 2009: Neogene glacigenic debris flows on James Ross Island, northern Antarctic Peninsula, and their implications for regional climate history. *Quaternary Science Reviews 28*, 3138–3160.

Nesov, L.A. 1991: Gigantskiye lyetayushchiye yashchyeryi semyeistva Azhdarchidae. I. Morfologiya, sistematika. *Vestnik Leningradskogo Universiteta, Seriya 7; Geologiya, Geografiya 2*, 14–23

Niklas, K.J. 1994: *Plant Allometry: the Scaling of Form and Process*. University of Chicago Press, Chicago.

O'Connor, J., Wang, X., Sullivan, C., Wang, Y., Zheng, X., Hu, H., Zhang, X. & Zhou, Z. 2018: First report of gastroliths in the Early Cretaceous basal bird *Jeholornis*. *Cretaceous Research 84*, 200–208.

Oloriz, F., Reolid, M. & Rodriguez-Tovar, F.J. 2004: Taphonomy of ammonite assemblages from the Middle-Upper Oxfordian (Transversarium?-Bifurcatus Zones) in the Internal Prebetic (Betic Cordillera, southern Spain): Taphonomic populations and taphofacies to support ecostratigraphic interpretations. *Rivista Italiana di Paleontologia e Stratigrafia, 110*, 239–248.

Packard, E.L. & Jones, D.L. 1962: A new species of *Anisoceras* from Oregon. *Journal of Paleontology 36*, 1047–1050.

Page, V.M. 1973: A new conifer from the Upper Cretaceous of central California. *American Journal of Botany 60*, 570–575.

Peecook, B.R. & Sidor, C.A. 2015. The first dinosaur from Washington State and a review of Pacific Coast Dinosaurs from North America. *PLoS One 10*, e0127792.

Pilkey, O.H., Morton, R.W. & Luternauer, J. 1967: The carbonate fraction of beach and dune sands. *Sedimentology 8*, 311–327.

Piper, D.Z., Loebner, B. & Aharon, P. 1986: Physical and chemical properties of the phosphate deposit on Nauru, western equatorial Pacific Ocean. *In* Notholt, A.J.G. (ed.), *Phosphate Deposits of the World*. Cambridge University Press, Cambridge, v. 3, p. 177–194.

Power, F.D. 1925: Phosphate deposits of the Pacific. *Economic Geology 20*, 266–281.

Reineck, H.E. & Singh, I.B. 2012. *Depositional Sedimentary Environments: With Reference To Terrigenous Clastics*. Springer, Berlin.

Retallack, G.J. 1984: Completeness of the rock and fossil record: some estimates using fossil soils. *Paleobiology 10*, 59–78.

Retallack, G.J. 1992: Middle Miocene fossil plants from Fort Ternan (Kenya) and evolution of African grasslands. *Paleobiology 18*, 383–400.

Retallack, G.J. & Dilcher, D.L. 2012. Outcrop versus core and geophysical log interpretation of mid-Cretaceous paleosols from the Dakota Formation of Kansas. *Palaeogeography, Palaeoclimatology, Palaeoecology 329*, 47–63.

Retallack, G.J., Theodor, J.M., Davis, E.B., Hopkins, S.S. & Barrett, P.Z. 2018: First dinosaur (Ornithopoda) from Early Cretaceous (Albian) of Oregon, U.S.A. *Journal of Vertebrate Paleontology 38*, https://doi.org/10.1080/02724634.2018.1486847

Sato, T. & Tanabe, K. 1998: Cretaceous plesiosaurs ate ammonites. *Nature 394*, 629–630.

Siversson, M. & Machalski, M. 2017: Late late Albian (Early Cretaceous) shark teeth from Annopol, Poland. *Alcheringa 41*, 433–463.

Skog, J.E. & Dilcher, D.L. 1994: Lower vascular plants of the Dakota Formation in Kansas and Nebraska, USA. *Review of Palaeobotany and Palynology 80*, 1–18.

Smith, A.B. & Rader, W.L. 2009: Echinoid diversity, preservation potential and sequence stratigraphical cycles in the Glen Rose Formation (early Albian, Early Cretaceous), Texas, USA. *Palaeobiodiversity and Palaeoenvironments 89*, 7–52.

Smith, K.T., Schaal, S.F.K. & Habersetzer, J. (eds) 2018: *Messel – An Ancient Greenhouse Ecosystem*. Schweitzerbartsche, Frankfurt.

Squires, R.L. & Saul, L.R. 2009: Cretaceous opine bivalves from the Pacific slope of North America and palaeobiogeography of subfamily Opinae Chavan, 1969. *Palaeontology 52*, 1311–1347.

Seuss, B., Wisshak, M., Mapes, R.H., Hembree, D.I., Landman, N. & Lignier, V. 2016: Microbial bioerosion of erratic sub-fossil *Nautilus* shells in a karstic cenote (Lifou, Loyalty Islands, New Caledonia). *Ichnos 23*, 108–115.

Szczuciński, W., Kokociński, M., Rzeszewski, M., Chagué-Goff, C., Cachão, M, Goto, K. & Sugawara, D. 2012. Sediment sources and sedimentation processes of 2011 Tohoku-oki tsunami deposits on Sendai Plain, Japan – insights from diatoms, nannoliths and grain size distribution. *Sedimentary Geology 282*, 40–56.

Surpless, K.D. & Gulliver, K.D.H. 2018: Provenance analysis of the Ochoco basin, central Oregon: A window into the Late Cretaceous paleogeography of the northern U.S. Cordillera. In Ingersoll, R.V., Graham, S.A., & Lawton, T.F. (eds), Tectonics, Sedimentary Basins, and Provenance: a Celebration of William R. Dickinson's Career. *Geological Society of America Special Paper 540*, 235–355.

Taylor, S.R. & McLennan, S.M. 1985: *The Continental Crust: its Composition and Evolution*. Blackwell, Oxford.

Underwood, C.J. 2004: Barremian and Aptian (Cretaceous) sharks and rays from Speeton, Yorkshire, NE England. *Yorkshire Geological Society Proceedings 55*, 107–118.

Walton, J. 1936: On the factors which influence the external form of fossil plants; with descriptions of the foliage of some species of the Palaeozoic equisetalean genus *Annularia* Sternberg. *Royal Society of London Philosophical Transactions B226*, 219–237.

Wani, R. 2004. Experimental fragmentation patterns of modern *Nautilus* shells and the implications for fossil cephalopod taphonomy. *Lethaia 37*, 113–123.

Wellnhofer, P. 1991: The skull of *Tapejara wellnhoferi* Kellner (Reptilia, Pterosauria) from the Lower Cretaceous Santana Formation of the Araripe Basin, Northeastern Brazil. *Mitteilungen der Bayerischen Staatssammlung für Paläontologie und Historische Geologie 31*, 89–106.

Welton, B.J. 1972: Fossil sharks in Oregon. *The Ore Bin 34*, 161–170.

Wendt, J. & Aigner, T. 1985: Facies patterns and depositional environments of Palaeozoic cephalopod limestones: *Sedimentary Geology 44*, 263–300.

Wilkinson, W.D. & Oles, K.F. 1968: Stratigraphy and paleoenvironments of Cretaceous rocks, Mitchell quadrangle, Oregon. *American Association of Petroleum Geologists Bulletin 52*, 29–16.

Williams, H.F. 2011: Shell bed tempestites in the Chenier Plain of Louisiana: late Holocene example and modern analogue. *Journal of Quaternary Science 26*, 199–206.

Wilson, M.A. 2007. Macroborings and the evolution of marine bioerosion. In Miller, W. (ed), Trace Fossils. Elsevier, Amsterdam, 356–367.

Yasukawa, K., Nakamura, K., Fujinaga, K., Machida, S., Ohta, J., Takaya, Y. & Kato, Y. 2015: Rare-earth, major, and trace element geochemistry of deep-sea sediments in the Indian Ocean: Implications for the potential distribution of REY-rich mud in the Indian Ocean. *Geochemical Journal 49*, 621–635.

Zatoń, M. & Salamon, M.A. 2008. Durophagous predation on Middle Jurassic molluscs, as evidenced from shell fragmentation. *Palaeontology 51*, 63–70.

Zuschin, M., Stachowitsch, M. & Stanton R.J. 2003. Patterns and processes of shell fragmentation in modern and ancient marine environments. *Earth Science Reviews 63*, 33–82.